

# Series expansion study of quantum percolation on the square lattice

 D. Daboul<sup>1,a</sup>, I. Chang<sup>2</sup>, and A. Aharony<sup>1</sup>
<sup>1</sup> School of Physics and Astronomy, Raymond and Beverly Sackler Faculty of Exact Sciences, Tel Aviv University, 69978 Tel Aviv, Israel

<sup>2</sup> Department of Physics, Pusan National University, Pusan 609-735, Korea

Received 28 February 2000

**Abstract.** We study the site and bond quantum percolation model on the two-dimensional square lattice using series expansion in the low concentration limit. We calculate series for the averages of  $\sum_{ij} r_{ij}^k T_{ij}(E)$ , where  $T_{ij}(E)$  is the transmission coefficient between sites  $i$  and  $j$ , for  $k = 0, 1, \dots, 5$  and for several values of the energy  $E$  near the center of the band. In the bond case the series are of order  $p^{14}$  in the concentration  $p$  (some of those have been formerly available to order  $p^{10}$ ) and in the site case of order  $p^{16}$ . The analysis, using the Dlog-Padé approximation and the techniques known as M1 and M2, shows clear evidence for a delocalization transition (from exponentially localized to extended or power-law-decaying states) at an energy-dependent threshold  $p_q(E)$  in the range  $p_c < p_q(E) < 1$ , confirming previous results (e.g.  $p_q(0.05) = 0.625 \pm 0.025$  and  $0.740 \pm 0.025$  for bond and site percolation) but in contrast with the Anderson model. The divergence of the series for different  $k$  is characterized by a constant gap exponent, which is identified as the localization length exponent  $\nu$  from a general scaling assumption. We obtain estimates of  $\nu = 0.57 \pm 0.10$ . These values violate the bound  $\nu \geq 2/d$  of Chayes *et al.*

**PACS.** 72.15.Rn Localization effects (Anderson or weak localization) – 05.70.Jk Critical point phenomena – 64.60.Ak Renormalization-group, fractal, and percolation studies of phase transitions

## 1 Introduction

Anderson localization [1] has been the subject of intensive studies for a long time, as a model for metal-insulator-transitions in disordered solids [2]. It is now well-established that for dimensions  $d \geq 3$ , there is a transition between extended and localized states, as the strength  $\lambda$  of the disorder increases. Above this transition ( $\lambda > \lambda_c$ ) all the electronic wave-functions are localized, namely, their envelope decays with distance  $r$  from the center as  $|\psi(r)| \sim \exp(-r/\xi(\lambda, E))$ , apart from power law pre-factors. The localization length  $\xi$  asymptotically diverges as  $\xi \sim (\lambda - \lambda_c)^{-\nu}$  as the threshold is approached. The one parameter scaling theory [3] for Anderson localization implies that this transition occurs above two dimensions (2D), while at and below 2D the wave-functions remain localized even for the smallest amount of disorder.

For several years interest has also focused on the quantum percolation (QP) problem [4–14], which is a variant of the Anderson model. Here a quantum mechanical entity (single electron) propagates, as governed by Schrödinger's equation in the tight binding representation, through a lattice in which a certain fraction  $q = 1 - p$  of sites or bonds have been blocked randomly. One of the main

concerns in the QP problem is to locate the percolation threshold  $p_q$ , below which all the eigenstates of the Hamiltonian are localized. For three dimensions (3D), numerical studies agree with each other and with the scaling theory on the existence of a transition ( $p_q < 1$ ), but the value of the exponent  $\nu$  has been the subject of much controversial discussion [9,10,12,13]. Chang *et al.* [9,10] obtained an estimate for  $\nu$  from series expansion which violates the bound  $\nu \geq 2/d$  by Chayes *et al.* [15]. Based on this finding the authors argued that the QP model belongs to a new universality class, different from that of the Anderson localization model. This new universality class may not fulfill the conditions needed for the Chayes *et al.* theorem to apply.

In 2D the situation is even more controversial. The same authors [10] and earlier Meir *et al.* [6] found evidence for a localization transition with  $p_q < 1$ , based on series expansion studies. This contradicts some numerical studies [7,11,16], but agrees with other studies, which use different numerical techniques and also find a transition [14,17–20].

This paper extends reference [10] for  $d = 2$ , in several directions. We now study the bond percolation case (BQP) with series of 14 terms in the concentration  $p$  for the quantities  $A_k$  for  $k = 0, 1, \dots, 5$ . These are the average

---

<sup>a</sup> e-mail: daboul@fractal.tau.ac.il

moments of inter-site distances, weighted by the transmission coefficients for quantum transmission between these pairs of sites:  $A_k = \left[ \sum_{ij} r_{ij}^k T_{ij}(E) \right]_p$  (for details refer to the following sections). We calculate and analyze these series for several values of the energy near the center of the band. We further add to our study the site percolation case (SQP) for which we generate new 16 term series for the same quantities. Unlike the various Monte Carlo simulation methods, the series method enumerates *exactly* all the configurations necessary up to a given order. The only approximation then involves the extrapolation of the series to infinite order, where one can use a large variety of well-established methods.

Section 2 gives the definitions of the model and of the quantities which we calculate, and explains how their power series are generated. In Section 3 we describe the process of series analysis. Section 4 discusses the results and gives our conclusion.

## 2 Quantum percolation model and generation of the series

The QP model is based on a tight binding Hamiltonian,

$$H = \sum_i \epsilon_i |i\rangle\langle i| + \sum_{\langle ij \rangle} v_{ij} (|i\rangle\langle j| + |j\rangle\langle i|), \quad (1)$$

where  $\langle ij \rangle$  denotes the pairs of nearest-neighbor (NN) sites and  $|i\rangle$  represents a tight binding basis wave function centered on site  $i$ . Like in the classical case, we define site and bond QP. In the SQP problem the on-site energies  $\epsilon_i$  are uncorrelated random variables, which assume the values 0 or  $\infty$  with respective probabilities  $p$  and  $1-p$ . Hence the propagating electron is completely forbidden to be on sites  $i$  with  $\epsilon_i = \infty$ , which we identify as vacant. All bonds are occupied ( $v_{ij} = 1$ ), allowing electron propagation between NN sites.

In the BQP problem we assume constant on-site energies  $\epsilon_i$ , which we take to be zero. Now the NN hopping matrix elements  $v_{ij}$  are uncorrelated random variables, which assume the values 1 or 0 with respective probabilities  $p$  and  $1-p$ . We refer to bonds for which  $v_{ij} = 0$  as vacant and to those with  $v_{ij} = 1$  as occupied. The SQP and BQP models are thus identified as tight binding models on site and bond percolation clusters.

To probe the localization transition, we start by considering an arbitrary pair of sites on the lattice,  $i$  and  $j$  (including the possibility  $i = j$ ). We next attach semi-infinite one-dimensional chains (in which all nearest neighbor  $v_{ij}$ 's are unity) to points  $i$  and  $j$ , insert an incoming wave  $e^{iqn}$  with energy  $E = 2 \cos q$  on the chain entering site  $i$ , and calculate the amplitude  $t_{ij}$  of the outgoing wave on the chain leaving from site  $j$ , by solving the QP model. Defining the corresponding transmission coefficient as  $T_{ij}(E) = |t_{ij}|^2$ , we next calculate the average transmission coefficient,

$$T(p, E) = \left[ \sum_{i,j} T_{ij}(E) \right]_p, \quad (2)$$

where the sum is over all pairs of lattice points, and  $[\dots]_p$  represents a configurational average over the  $v_{ij}$ 's in the bond case or over the  $\epsilon_i$ 's in the site case. In the following we give the explanations for the bond problem only, but the generalization for site percolation should be obvious.

A generalization of  $T(p, E)$  involves the moments of distances between pairs of lattice sites,

$$A_k(p, E) = \left[ \sum_{i,j} r_{ij}^k T_{ij}(E) \right]_p, \quad (3)$$

where  $r_{ij}$  denotes the geometrical distance between sites  $i$  and  $j$ . Clearly,  $T(p, E) = A_0(p, E)$ . We study these moments up to order  $k = 5$ , to obtain estimates for the localization length exponent  $\nu$ . This is based on the following scaling assumption: For small  $p$ , we expect that in some average sense  $[T_{ij}(E)]_p \sim r_{ij}^{-c} f(r_{ij}/\xi)$ , where  $c > 0$  and  $f(x)$  is a scaling function which approaches a constant as  $x \rightarrow 0$  and decays exponentially for  $x \rightarrow \infty$ . Therefore

$$\begin{aligned} A_k(p, E) &\sim \int r_{ij}^k [T_{ij}]_p d^d r_{ij} \sim \int r^{k-c} f(r/\xi) d^d r \\ &\sim \xi(p, E)^{d-c+k} \int x^{k-c} f(x) d^d x \\ &\sim (p_q - p)^{-\nu(d-c+k)} \sim (p_q - p)^{-\gamma - k\nu}, \end{aligned} \quad (4)$$

with  $\gamma = \nu(d-c)$ .

Given the concentration  $p$  of conducting bonds, each realization of the system consists of clusters ( $\Gamma$ ) of sites interconnected by conducting bonds. For small  $p$ , the average  $[\dots]_p$  may be expressed as a sum over the clusters [21],

$$A_k(p, E) = \sum_{\Gamma} p^{n_b(\Gamma)} (1-p)^{n_p(\Gamma)} \sum_{i,j \in \Gamma} r_{ij}^k T_{ij}(E), \quad (5)$$

where  $n_b(\Gamma)$  and  $n_p(\Gamma)$  are the numbers of bonds in  $\Gamma$  and on its perimeter. If  $T_{ij}$  is replaced by 1 for all  $i$  and  $j$  in  $\Gamma$ , then (2) reduces to the mean cluster size  $S$  and (3) reduces to the  $k$ th moment of the correlation length of classical percolation, both diverging at the classical percolation threshold  $p_c$  [22].

Since the sum in (5) contains polynomials in  $p$ , the averages in (2) and (3) yield series in  $p$ . A calculation to order  $p^n$  involves all clusters with up to  $n$  bonds. The series for  $T$  require only the topology of the clusters. In contrast,  $A_k$  depends on the explicit geometry of each cluster, which requires much more data. Separate computer programs [23] were used to enumerate all different cluster configurations recursively, by an algorithm similar to those described in [24–26]. These programs store the necessary information in shape data-files which include clusters with up to 14 bonds or up to 16 sites, respectively. The data have been used previously in [27], where some discussion on checks of their correctness is given.

With the list of graphs available, what remains to be done in order to obtain the series for  $T$  or  $A_k$  according to (5) and (3), is to calculate the  $T_{ij}$ 's for all the graphs. For bond percolation [5, 10] give some details on how this calculation is done. Here we will complement this information

$$\begin{pmatrix} \ddots & \vdots \\ \dots & -E & 1 & 0 & 0 & 0 & 0 & 0 & 0 & 0 & 0 & \dots \\ \dots & 1 & -E & 1 & 0 & 0 & 0 & 0 & 0 & 0 & 0 & \dots \\ \dots & 0 & 1 & -E & 1 & 0 & 0 & 0 & 0 & 0 & 0 & \dots \\ \dots & 0 & 0 & \boxed{1} & \boxed{-E} & \boxed{1} & \boxed{0} & \boxed{1} & \boxed{0} & 0 & 0 & \dots \\ \dots & 0 & 0 & 0 & 1 & -E & 1 & 0 & 0 & 0 & 0 & \dots \\ \dots & 0 & 0 & 0 & 0 & 1 & -E & 1 & 0 & 0 & 0 & \dots \\ \dots & 0 & 0 & 0 & 1 & 0 & 1 & -E & 1 & 0 & 0 & \dots \\ \dots & 0 & 0 & 0 & 0 & 0 & 0 & 1 & -E & 1 & 0 & \dots \\ \dots & 0 & 0 & 0 & 0 & 0 & 0 & 0 & 1 & -E & 1 & \dots \\ \dots & 0 & 0 & 0 & 0 & 0 & 0 & 0 & 0 & 1 & -E & \dots \\ \vdots & \ddots & \ddots \end{pmatrix} \begin{pmatrix} \vdots \\ \psi_{-4} \\ \psi_{-3} \\ \psi_{-2} \\ \psi_{-1} \\ \psi_a \\ \psi_b \\ \psi_{+1} \\ \psi_{+2} \\ \psi_{+3} \\ \psi_{+4} \\ \vdots \end{pmatrix} = 0. \tag{6}$$

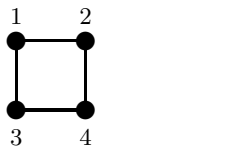


Fig. 1. Example cluster: square plaquette.

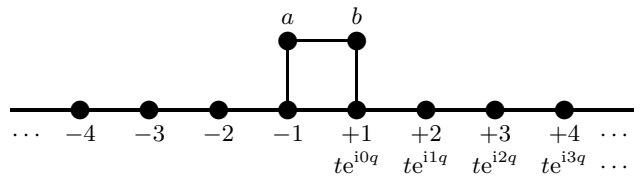


Fig. 2. Infinite chains connected to 2 different sites of the cluster.

by showing how to set up the tight binding Hamiltonian in the site percolation case for the example cluster shown in Figure 1. For a particular transmission coefficient we simplify the Schrödinger equation for the cluster with attached chains, and end up with a set of linear equations that can be solved to yield  $T_{ij}$  by standard techniques.

We now demonstrate this calculation by deriving  $T_{-1,1}$  for Figure 2. With the site-labeling as given in the figure, we write down the relevant part of the Schrödinger equation  $H\Psi = E\Psi$  in the site basis:

see equation (6) above.

We simplify this infinite matrix problem to a finite one, using the Ansatz

$$\begin{aligned} \psi_{-(n+1)} &= e^{-inq} + re^{inq} \\ \psi_{(n+1)} &= te^{inq}, \end{aligned}$$

( $i = \sqrt{-1}$ ) for  $n = 0, 1, \dots$ . This Ansatz is of course identified as an incoming wave from the left, which is partly transmitted to the right, but also partly reflected back. The amplitudes on the outgoing chain are written down explicitly in Figure 2. On inserting the above Ansatz into (6) one verifies that it satisfies the equations on the chains with the well-known relation between  $q$  and  $E$ ,

$$e^{-iq} + e^{iq} = E \iff q = \arccos(E/2),$$

which imposes on  $E$  the 1D energy band limits  $-2 \leq E \leq 2$ .

We are now left with a finite system of linear equations, corresponding to the inner box in (6),

$$\begin{pmatrix} -E + e^{iq} & 1 & 0 & 1 \\ 1 & -E & 1 & 0 \\ 0 & 1 & -E & 1 \\ 1 & 0 & 1 & -E + e^{iq} \end{pmatrix} \begin{pmatrix} 1 + r \\ \psi_a \\ \psi_b \\ t \end{pmatrix} = \begin{pmatrix} e^{iq} - e^{-iq} \\ 0 \\ 0 \\ 0 \end{pmatrix}. \tag{7}$$

It involves only sites on the cluster, can be solved for  $t \equiv t_{-1,+1}$ , and the desired transmission coefficient  $T_{-1,+1} = t^*t$  is obtained. In the computerized calculation one would now refer to the data-files to obtain the number of cluster sites  $n_s$ , the site perimeter  $n_p$ , and the geometrical site distances  $r_{ij}$ , and combine those to get the cluster’s contribution to the series, according to (5). For our example,  $n_s = 4$ ,  $n_p = 8$ , and  $r_{ij} = 0, \sqrt{2}$ , or 1.

Tables 1 and 2 list the coefficients in the power series for  $E = 0.05$ , the energy value we studied most extensively.

### 3 Analysis of the series

As explained below, our analysis used the Dlog-Padé method [28] and the methods M1 and M2 [29,30]. All of these were combined with Euler-transformations for improved results. For each series, our main goal was to obtain the critical threshold  $p_q$  and the critical exponent which describe the expected power law divergence as in (4). Having followed this for several energies, we present detailed

**Table 1.** Series for bond quantum percolation at  $E = 0.05$ .

Coefficients $a_n$ in $\dots = \sum_n a_n p^n$			
$n$	$T(p)$	$A_1(p)$	$A_2(p)$
0	1.0000000000000000	0.0000000000000000	0.0000000000000000
1	0.03957945284315	4.0000000000000000	4.0000000000000000
2	6.0074156477499	-4.448814783956	8.2374767170589
3	-14.6523834314562	50.8004930461771	40.6487625304979
4	90.379666362283	-187.719303537795	9.042112348758
5	-397.05721237573	1068.2863925791	417.81036532941
6	1985.4017604669	-5207.4605890481	-1057.8566333405
7	-9616.769785599	27070.96616584	7204.497199292
8	47458.19229530	-138440.41197483	-32238.163905991
9	-233579.5799124	715329.7867960	170992.9117054
10	1150445.233208	-3697482.86660	-869805.429016
11	-5646077.00459	19173708.14468	4608254.9866
12	27565972.46187	-99641486.7740	-24814011.855
13	-133538213.9423	519169541.7114	137475024.677
14	639926553.90	-2712719744.041	-782576209.09

Coefficients $a_n$ in $\dots = \sum_n a_n p^n$			
$n$	$A_3(p)$	$A_4(p)$	$A_5(p)$
0	0.0000000000000000	0.0000000000000000	0.0000000000000000
1	4.0000000000000000	4.0000000000000000	4.0000000000000000
2	30.86489371502841	72.2374767170589	149.4923107129979
3	81.748745414783	301.714932494421	1079.43245514488
4	320.99465308520	1163.50160575778	4552.3161589277
5	363.1577941159	2763.0007578961	15747.841405944
6	3002.304839285	10246.191812356	46602.12045721
7	-4477.05338451	9852.511059961	127518.9407191
8	45676.7818067	92341.48575417	300318.983304
9	-182685.994932	-130494.9602474	830627.10615
10	983094.74967	1210064.19908	848221.143
11	-4418711.64120	-3365966.8395	11646458.19
12	19156449.7128	7781630.62	-73117818.05
13	-66359167.688	70124104.1	794289573.1
14	97892791.6	-1197379145.3	-7155423404.7

results for all the series  $A_0$  to  $A_5$ , both in bond and site percolation, at  $E = 0.05$ , and in the BQP case also for  $E = 0.07$ .

In addition to fitting our series to power law divergences, as in (4), we also followed Soukoulis and Grest [7] and attempted fitting the localization length to the form

$$\xi(p) = A \exp\left(B \left(\frac{p}{1-p}\right)^y\right), \tag{8}$$

which would imply a threshold  $p_q = 1$ , namely no transition. As we discuss below, this latter form does not fit our series.

### 3.1 Dlog-Padé analysis

The Dlog-Padé method is one of the most common methods for the asymptotic analysis of series. One calculates Padé approximants to the logarithmic derivative of the series and obtains estimates for the critical threshold ( $p_q$ ) and exponent ( $\gamma + k\nu$ ) from their real first order poles and the corresponding residues. In the following we will refer to each such pole-residue-pair as a data-point; these points are often plotted in a diagram of residues *versus* poles.

The coefficients  $a_n$  of our series start to alternate in sign above a certain  $n$ , suggesting that the  $A_k$ 's have a singularity on the negative axis. This was confirmed by

**Table 2.** Series for site quantum percolation at  $E = 0.05$ .

Coefficients $a_n$ in $\dots = \sum_n a_n p^n$			
$n$	$T(p)$	$A_1(p)$	$A_2(p)$
0	0.0000000000000000	0.0000000000000000	0.0000000000000000
1	1.0000000000000000	0.0000000000000000	0.0000000000000000
2	0.03957945284315	4.0000000000000000	4.0000000000000000
3	6.0074156477499	-4.44881478395635	8.2374767170589
4	-15.0283251433228	43.7146422699542	40.499242290840
5	68.25139563829	-135.665100908902	6.64882296999
6	-250.010808280226	620.9710988777	298.67018968013
7	1010.25028610076	-2432.377356234	-603.389626813
8	-3989.9567096966	10103.902081227	3431.316029343
9	15921.637061458	-41007.625589472	-12107.995039736
10	-63170.64881925	167709.66323635	51624.65390381
11	250361.97242683	-683832.2855886	-206522.3184462
12	-988074.3391790	2792714.8675073	864511.977329
13	3877641.328297	-11414962.4492	-3664978.349064
14	-15099633.0805	46756660.7835	16050060.7665
15	58219742.9450	-192049761.5717	-72455863.605
16	-221615389.799	791818339.302	337957457.51

Coefficients $a_n$ in $\dots = \sum_n a_n p^n$			
$n$	$A_3(p)$	$A_4(p)$	$A_5(p)$
0	0.0000000000000000	0.0000000000000000	0.0000000000000000
1	0.0000000000000000	0.0000000000000000	0.0000000000000000
2	4.0000000000000000	4.0000000000000000	4.0000000000000000
3	30.86489371502841	72.23747671705889	149.49231071299793
4	91.4086778930381	325.2475260458056	1122.58395413209
5	293.35018871584	1229.04360113283	5064.2307347288
6	440.4534408151	2935.61054030906	17128.783407173
7	1698.0041410811	8405.952345506	47775.69791875
8	-29.878237684	12601.91377327	120339.37647009
9	12804.79044742	45788.0529727	261175.6691200
10	-29129.1612421	8663.608786	600274.009761
11	147955.223726	287870.520363	856298.66374
12	-454712.47646	-214507.6219	4345569.4898
13	1314081.6792	-400178.1236	-14365480.90
14	-792537.7645	20592040.366	152270963.96
15	-24640151.570	-194727776.05	-1082292395.
16	272899691.18	1528906185.8	7882563835.

our Dlog-Padé analysis. Application of Euler-transformations, into the new variables  $z = p_n p / (p_n - p)$ , with  $p_n$  near  $-0.2$ , usually improved the behavior of the transformed series.

For SQP we obtain satisfactory results in this manner. Data points in the pole residue plot are high in number (above 50) and well concentrated along a distinct line for each series. Figure 3 shows the  $p_q$  and exponent estimates as function of a parameter which represents the order of the corresponding Padé approximant. As seen from this figure, the estimates appear to converge for most series. Therefore, we decided to calculate results for the critical parameters as averages over the points of higher order, with error margins set by the standard deviation  $\sigma_N$ . Points included in the average are surrounded by a box in Figure 3, and their number is in the range of  $42 \pm 10$ . In Figure 4 we plot the resulting  $p_q$ 's and exponents as a function of  $k$ . The slope of the linear fit in Figure 4b suggests  $\nu = 0.70$ , the error bars on the individual points allow some variation not exceeding  $0.5 < \nu < 0.75$ . The overall threshold estimate from this Dlog-Padé analysis is  $p_q = 0.74 \pm 0.03$ .

In the bond case however, the Dlog-Padé method, even in combination with an Euler-transformation, showed to be insufficient for a quantitative analysis. As  $k$  in  $A_k$  increases, the suggested  $p_q$ , determined as some average over data points, appears to grow (roughly  $p_q = 0.64, 0.65, 0.68, 0.68, 0.69, 0.71, 0.72$  for  $k = 0 \dots 6$  and  $E = 0.05$ ). Acceptance of such an erroneous  $p_q$  would also predict a much larger exponent  $\nu \approx 1$  (leading exponents for  $A_k$  of roughly 1.3, 2.1, 3.2, 3.8, 5.0, 6.4, 7.6 for  $k = 0 \dots 6$ ). A biased reading at the presumably correct  $p_q$  (determined later) does not seem satisfactory either, since for some series only a negligible number of points are located in that area. Accordingly in the bond percolation case we use the Dlog-Padé method only to get rough estimates for the critical parameters as a starting point for M1 and M2, and to assess the general behavior of the series from the number of pole-residue pairs which are obtained.

### 3.2 Estimation of $p_q$ and critical exponents using M1 and M2

The analysis algorithms M1 and M2 allows the accurate simultaneous determination of the threshold  $p_q$ , leading critical exponent (denoted by  $h$  in general), and confluent correction to scaling exponent  $\Delta_1$ , assuming the asymptotic form

$$A(p_q - p)^{-h} (1 + B(p_q - p)^{\Delta_1}).$$

In both methods one finds the point of best convergence in the  $(p_q, h, \Delta_1)$  space, by examination of 2D plots at different trial values for  $p_q$  [30]. The effectiveness and preciseness of these series analysis methods has been demonstrated in several papers [21, 29, 31, 32].

For the accurate determination of the critical properties we concentrated on the energy values  $E = 0.05$ , which

has also been used in previous publications [6, 9, 10], and  $E = 0.07$  (bond case). In cases where we looked at other energies, the results were similar.

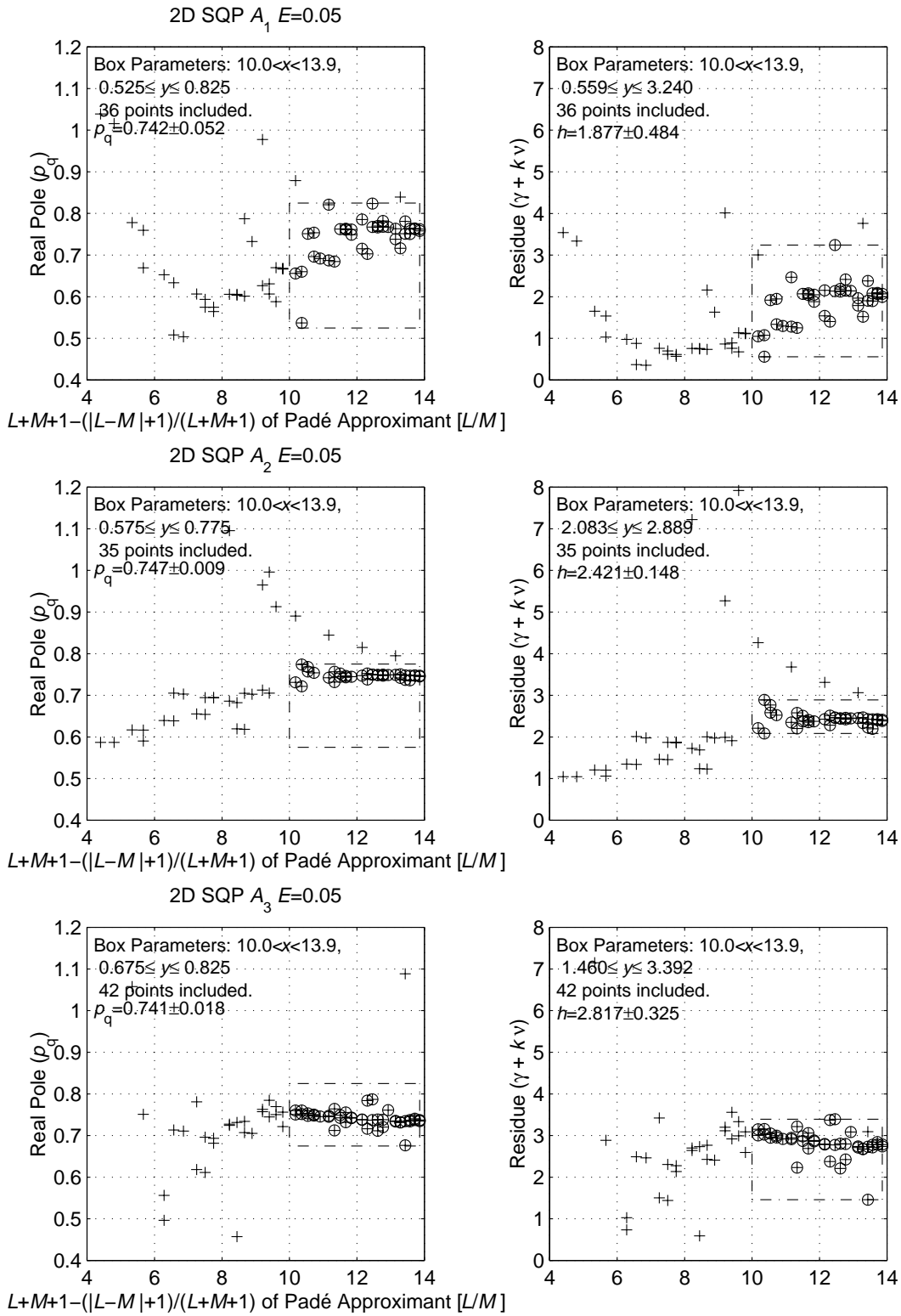
First we determine for each series separately the triple  $(p_q, h, \Delta_1)$  of best convergence. Using M1 this was always possible, with the exception of  $A_1$  in the bond percolation case. The trial- $p_q$  is varied until best convergence and symmetry of the curves from all high order Padé approximants is obtained. This  $p_q$  and the corresponding  $h$  are taken as the temporary best estimates for that series, with temporary error estimates from the nearest trial- $p_q$ 's, whose plots show poorer convergence. In many cases M1 proves to be quite sensitive to small changes in the trial- $p_q$ , and the degree of convergence usually looks very convincing. Away from the best  $p_q$ , convergence degrades quickly, the picture becomes unsymmetric and at the same time the area of convergence shifts to lower or higher values of  $h$ . We show examples of such plots in Figures 5 and 6.

In comparison, the M2-plots are in many cases much less decisive. The well-converged crossing of Padé approximant curves, expected for the best choice of  $p_q$ , sustains over a much wider range, where again the change in  $p_q$  is accompanied by a shift in the corresponding  $h$ . In such cases we only made sure that the estimate from M1 is in agreement with the M2-plots, but did not attempt to decide separately on best estimates from M2. We show examples of M2-plots in Figures 7 and 8.

Next we construct an overall estimate for  $p_q$  (with symmetric error bars), as to be consistent with the estimates from all individual series. We then look again at plots from M1 and M2 at the trial- $p_q$ 's set by the overall  $p_q$  bounds. In some cases this requires an increase in the error estimates for the leading exponent.

The leading exponent values for  $A_k$  are plotted as function of  $k$  in Figures 9 and 10 for the bond and site cases, respectively. No estimate for  $A_1$  in bond percolation could be obtained, due to lack of convergence. According to our scaling assumption (Sect. 2) all points should lie on a single straight line, with slope  $\nu$ . Apart from  $A_2$  in the bond case, the data comply very well with this prediction. Final  $\nu$ -estimates are obtained from the range of slopes which produce lines passing through all points within their error bounds. ( $A_2$  in the bond case was excluded.)

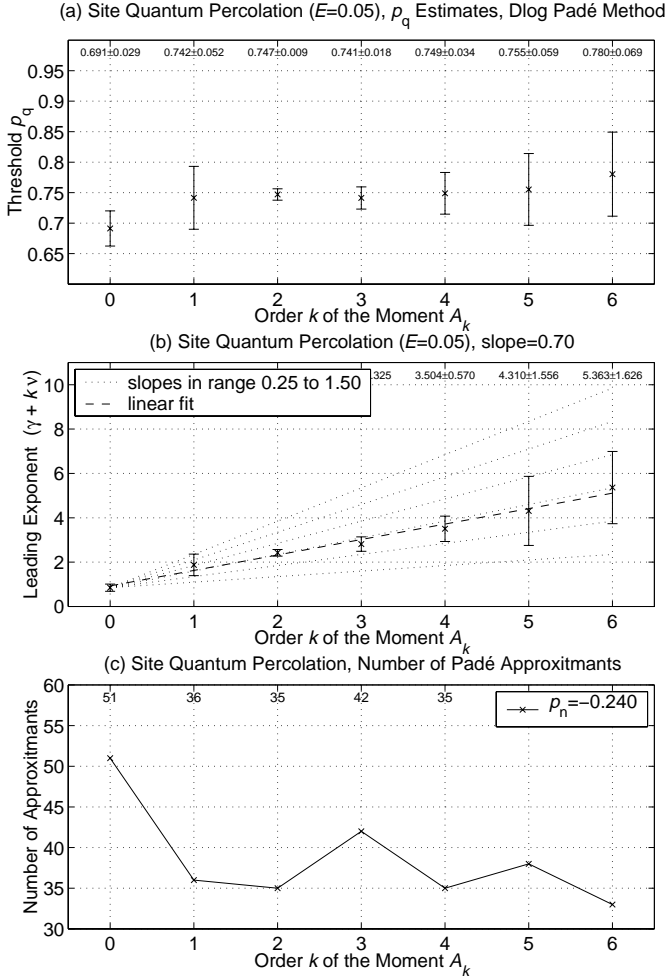
The numerical results are summarized in Table 3. In this table we also include (in parentheses) estimates for  $\gamma$  and  $\Delta_1$ . The critical exponent  $\gamma$  for the average transmission coefficient  $T$  is related to the decay rate of  $T_{ij}$  as  $r_{ij}^{-c}$ , see (4). Thus, our rough estimate  $\gamma \approx 1$  implies that  $c = d - \gamma/\nu \approx 0$ , *i.e.*  $T_{ij}$  decays very slowly at  $p_q$ . Our estimates for the correction exponent  $\Delta_1$  are even rougher, as we did not perform a dedicated study aimed to determine them accurately. The Table just lists the range of values deduced from the M1 and M2 analyses. We comment that the Euler transformations are known to produce analytic correction terms even if not present originally. When the leading correction exponent is larger than 1, as seems to be the case here, these "artificial" corrections will show up in M1 and M2 [33], and hence our  $\Delta_1$  estimates do



**Fig. 3.** Dlog-Padé analysis of the series  $A_1$ ,  $A_2$ , and  $A_3$  for SQP. An Euler transformation with  $p_n = -0.24$  was applied. The numbers on the  $x$ -axes represent the order of the Padé approximant, and are close to the length of the series used.

**Table 3.** Summary of the critical parameters.

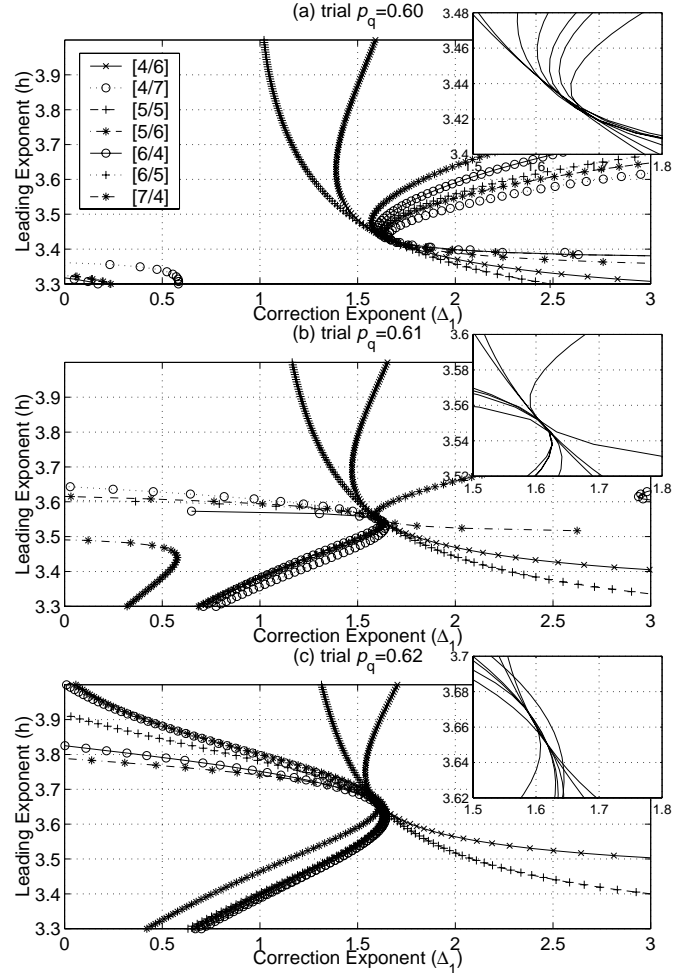
model	$E$	$p_q$	$\nu$	$\gamma$	$\Delta_1$
BQP	0.05	$0.625 \pm 0.025$	$0.51 \pm 0.05$	$(\approx 1)$	$(\approx 1 \dots 1.7)$
BQP	0.07	$0.590 \pm 0.020$	$0.49 \pm 0.04$	$(\approx 1.1)$	$(\approx 1.1 \dots 1.6)$
SQP	0.05	$0.740 \pm 0.025$	$0.61 \pm 0.06$	$(\approx 1)$	$(\approx 1 \dots 2)$

**Fig. 4.** Results for the critical parameters in SQP from Dlog-Padé analysis.

not have much significance. The stated ranges include the estimates from all individual series.

### 3.3 Sensitivity to the Euler transformation

Our analysis relies in a large part on the use of Euler transformations to increase the number of useful Padé approximants and to improve their convergence. The technique is well-established and has been used with success [34], but nevertheless we found it worthwhile to check, to what degree our results are sensitive to the precise choice of  $p_n$ , the value of  $p$  which is mapped to infinity by the Euler transformation. We first chose a  $p_n$  very close to the

**Fig. 5.** M1 analysis of the series  $A_5(p)/p$  for BQP ( $E = 0.05$ ). Plots for different trial values of  $p_q$ . The best values for  $h$  and  $p_q$  are found from the crossing of all the Padé approximants. The central one (b) shows best convergence and symmetry of the curves resulting from the different Padé approximants. Indices are given in the legend. An Euler transformation with  $p_n = -0.2$  was applied. The insets show enlarged views of the convergence region. The deduced values  $p_q = 0.61 \pm 0.01$ ,  $h = \gamma + 5\nu = 3.55 \pm 0.10$  and  $\Delta_1 = 1.6 \pm 0.1$  further take into account the analysis with M2 and different  $p_n$ .

negative singularity, as indicated by the Dlog-Padé analysis of the original series. We then varied this  $p_n$  over a considerable range of typically 10 to 20%, and compared the results. We observed that a variation of  $p_n$  does move the data points or curves obtained from individual Padé approximants, but that the average (in Dlog-Padé plots)

**Table 4.** Overview over the energy dependence for the Dlog-Padé analysis in BQP.

Energy	Rating	Comments on behavior of the series
0.01	0	
0.02	2	$A_4$ about 30 data points, $A_1, A_2$ unusual high $p$ values (0.8–0.9), $T, A_3, A_5$ bad.
0.03	3	Only $A_1, A_2$ with 50 data points, others worse as for $E = 0.02$ .
0.04	4	50 to 60 data points for $T$ to $A_4$ in a wider range (0.3 in $p$ ), $A_5$ bad.
0.05	5	40 to 70 data points for $T$ to $A_4$ , $A_5$ only 20, $p_q$ shifts up with increasing order $k$ in Dlog-Padé analysis.
0.06	5	40 to 70 data points for $T$ to $A_4$ , $A_5$ only 20, $p_q$ shifts up with increasing order $k$ in Dlog-Padé analysis.
0.07	5	40 to 60 data points for $T, A_1, A_3, A_4$ , $A_2$ less, $A_5$ only 20, $p_q$ shifts up with increasing order $k$ in Dlog-Padé analysis.
0.08	4	30 to 40 data points for each series, except for $A_5$ being worse.
0.09	3	20 to 40 data points for each series.
0.1	1	Only about 20 data points within a reasonable region.
0.5	0	

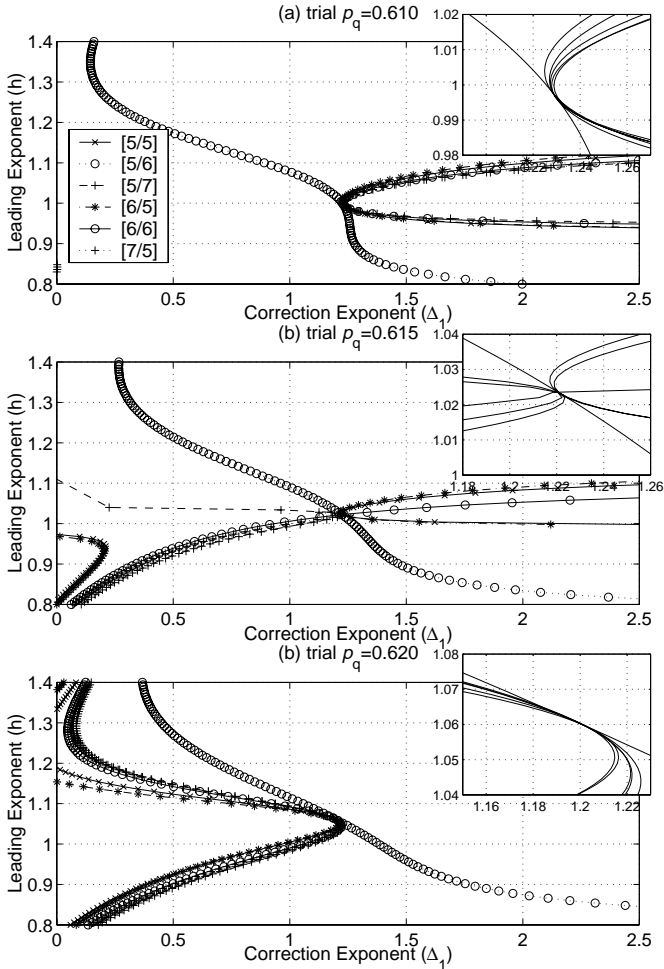


**Fig. 6.** M1 analysis of the series  $T(p)$  for BQP. ( $E = 0.05$ ). Plots for different trial values of  $p_q$ . The central one (b) shows best convergence and symmetry of the curves resulting from the different Padé approximants. Indices are given in the legend. An Euler transformation with  $p_n = -0.2$  was applied. The insets show enlarged views of the convergence region. The deduced values  $p_q = 0.61 \pm 0.01$ ,  $h = \gamma = 1.00 \pm 0.15$  and  $\Delta_1 = 1.25 \pm 0.20$  further take into account the analysis with M2 and different  $p_n$ .

and the convergence region (in M1 plots) stay fixed to very good accuracy, when compared to the error bounds given by the analysis technique itself. We illustrate this in Figures 11a–11c. We are therefore convinced that we can exclude the possibility that our results are artifacts of the applied Euler transformations.

### 3.4 Study of energy dependence

The energy band for the periodic square lattice (all  $v_{ij} = 1$  and  $\epsilon_i = 0$  in the Hamiltonian (1)) is  $[-4, 4]$ . It is expected [35], and confirmed by numerics [36], that these limits also apply (at least approximately) to possible extended states in the presence of disorder. The semi-infinite chains, which we use to define the transmission coefficients, impose the band limits  $[-2, 2]$  of the 1D-case on the range of Bloch waves which can be injected into the system. This limitation can be overcome by choosing a different value  $v_{ij} \neq 1$  for the hopping amplitudes on those chains. However, we have not done this, since we are only interested in states near the band center, which are expected to be the first to de-localize with increasing  $p$ .

We generated series for different energies, aiming to check to what degree our results depend on this parameter and possibly gain insight into the  $E$ -dependence of the quantum threshold  $p_q$ . In this part of the study we concentrate on the bond case.

The results from the Dlog-Padé analysis reveal that the series behave well only in a very narrow energy region. From the number of pole-residue pairs and from the quality of their convergence we subjectively rated the series for the different energies with grades from 0 (worst) to 5 (best behavior), and summarize in Table 4. This rating does not always apply to all the moments, but rather gives an average. When the quality of convergence varies for the moments ( $T, A_1, \dots, A_5$ ),  $A_5$  usually performs relatively bad.

The energy region of good convergence  $E = 0.04$  to  $0.08$  is small compared to the width of the energy band. As a general feature, we observe without exception, that the line of pole-residue points shifts to smaller  $p_q$  and/or exponents for increasing energy. From the Dlog-Padé analysis

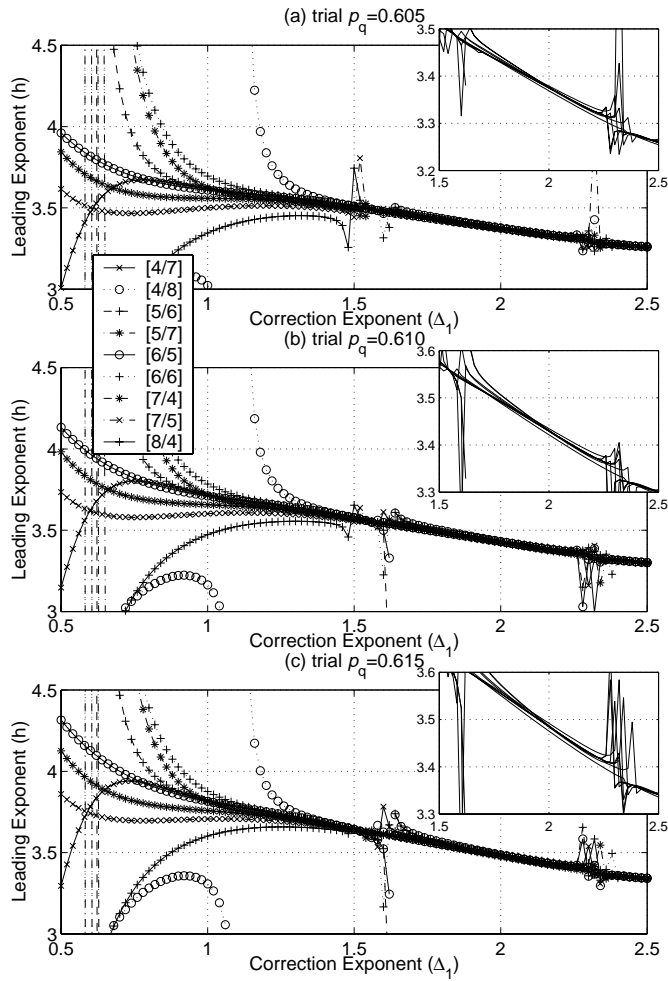


**Fig. 7.** M2 Analysis of the same series as used for Figure 5. An Euler Transformation with  $p_n = -0.2$  was applied. We see no drastic changes in the convergence but a general agreement with M1.

alone we cannot give much importance to this tendency. As mentioned above, such plots also seem to shift to larger  $p_q$  for increasing order  $k$  of the moments. The latter shifts were resolved when applying M1 and M2. The results from a study with M1 and M2 show no systematic changes in the leading exponent, and the related shifts in  $p_q$  over the narrow energy range are too small to draw detailed conclusions. The  $p_q$  estimates for  $E = 0.05$  and  $E = 0.07$  are centered at 0.625 and 0.590, but still overlap within their error bars (Tab. 3). We conclude that at present not much insight can be gained from the series, concerning the  $p$ -dependence of the mobility edge.

### 3.5 Checks for an essential singularity

Based on the transfer-matrix technique and finite-size scaling, Soukoulis and Grest [7] fitted their data to a divergence of the localization length as in (8), with  $y$  very close to 0.5. Such a divergence should carry over to the moments  $A_k$ , for  $k > 0$ .

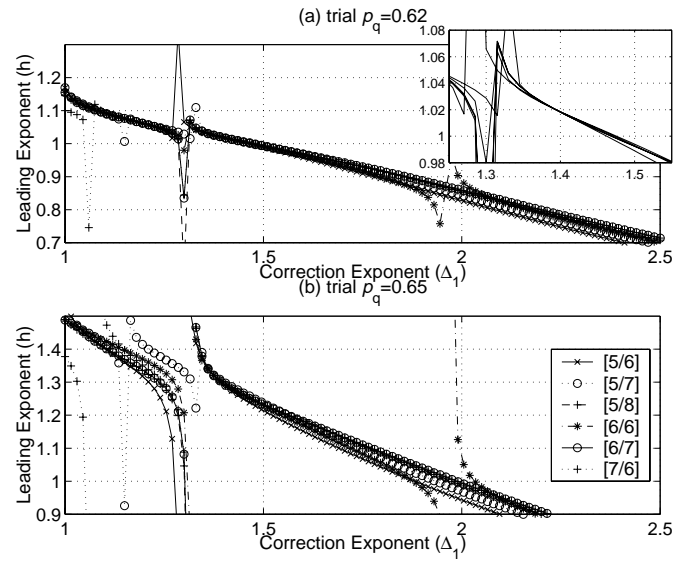


**Fig. 8.** M2 analysis of the series  $T(p)$  for BQP ( $E = 0.05$ ). Plots for different trial values of  $p_q$ . The upper one (a) shows best convergence of the curves resulting from the different Padé approximants. Indices are given in the legend. An Euler transformation with  $p_n = -0.2$  was applied.

To check whether our series could in fact describe such an essential singularity, instead of the proposed power law  $(p_q - p)^{-h}$ , we first calculate the series for the logarithmic derivative of the original quantity, and then apply all of our regular analysis techniques to these series. According to the above functional forms, these derived series should give us a regular power law singularity with the exponent  $y + 1 \approx 1.5$  at  $p = 1$  in the first case, or the exponent 1 at  $p = p_q$  in the second case.

The analysis of the so-transformed series proved difficult, because the additional logarithmic derivative produced new singularities near the origin, and these badly influenced the behavior. In most cases this could be alleviated by proper Euler transformations, typically applied after taking the first logarithmic derivative.

In no case did the series support the form of divergence (8). Very few data points (or none) were found in the relevant region of the Dlog-Padé plots, and no convergence was obtained in M1 and M2.

Within the limitations set by the poorer behavior, we obtained, for most series, plots which did support the power law divergence of  $\xi$ , namely were in agreement with poles near the proposed  $p_q$  together with a residue close to 1. As a typical example we show such plots for  $A_2$  in the bond percolation case (Figs. 12–15). For comparison we also show an M1-plot at a trial- $p_q$  of 1. While the results from this sub-section may not be convincing alone, they do support the evidence for the power law divergences of the  $A_k$ 's.

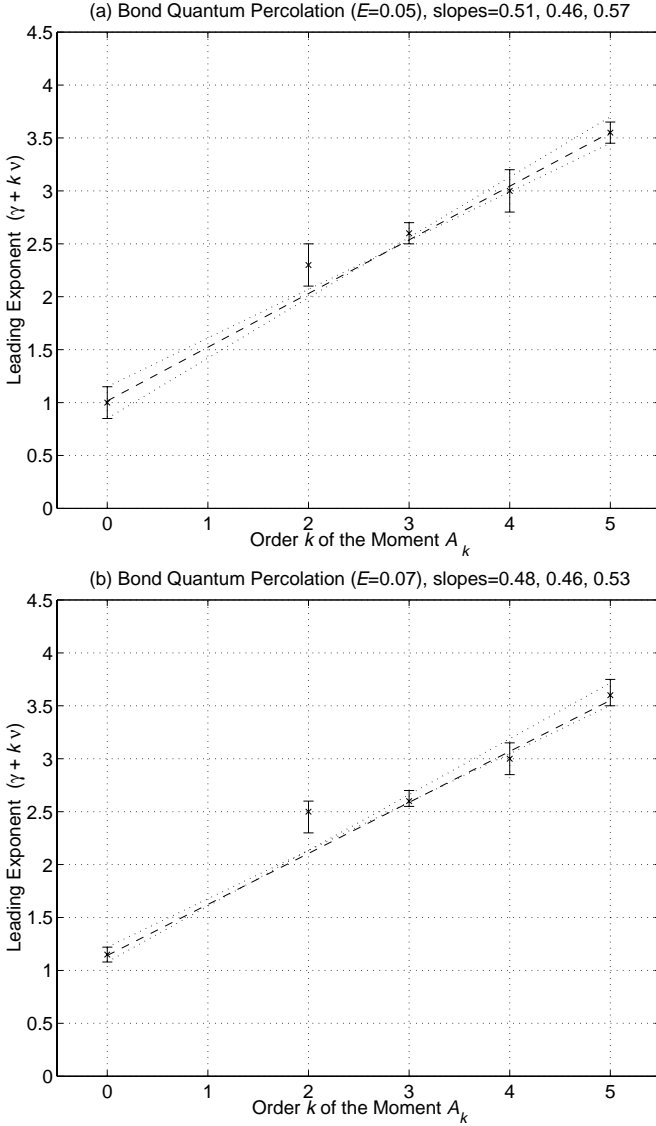


**Fig. 9.** Plots of the leading exponent for the moments  $A_k(p)$  versus  $k$  for the bond percolation case, (a)  $E = 0.05$ , (b)  $E = 0.07$ . They are expected to fall on a straight line, with slope  $\nu$  (localization length exponent). Error bounds for  $\nu$  are determined from the range of possible slopes. No estimates were obtained for  $A_1$ .

## 4 Summary of results and discussion

In the preceding sections we presented results from our recent numerical study of two-dimensional site and bond quantum percolation. Table 3 summarizes the quantitative results. While the study in part gives very convincing evidence for a de-localization transition, it also leaves room for some doubts. On the positive side, we list that

- We find a common quantum percolation threshold  $p_q$  for all series within one model, within reasonable error margins.

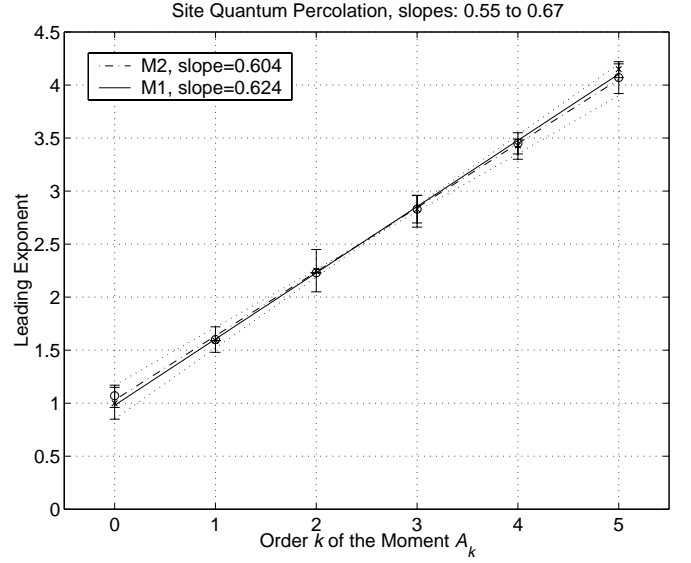


**Fig. 10.** Plot analogous to Figure 9 but for the site percolation case.

- We find that  $p_q$  is larger for the site case than for the bond case, as would be expected from the thresholds for classical geometrical percolation.
- We find a constant gap exponent for the moments  $A_k$ , consistent with the scaling assumption, and the points in Figures 9 and 10 fall well on a straight line.
- The results from the previously existing 10-term series for bond percolation have been confirmed by the newer 14-term series.

On the down-side, we note that

- The bond percolation series do not behave well enough to give consistent results with a regular Dlog-Padé analysis, which could imply that the correction to the leading exponent plays a sufficient role to destroy proper convergence (if not accounted for). M1 and M2 do not suffer from the problem observed with Dlog-Padé analysis.
- We find only marginal agreement on a common  $\nu$  from bond and site percolation. However, the stated error estimates are not rigorous bounds, and the result from the longer and better behaved site-percolation series are probably more trustworthy.
- the attempted study of the energy dependence revealed only a narrow region in which the series behave sufficiently well.

In addition there are the usual limitations of all series expansion studies. The analysis necessarily includes assumptions about the critical behavior, which, in the case under study, may need further justification. The possibility remains that the series may still be too short to reveal the correct parameters, even if the correct assumptions are made. Given these limitations one should be cautious to draw conclusions on the critical behavior from series alone.

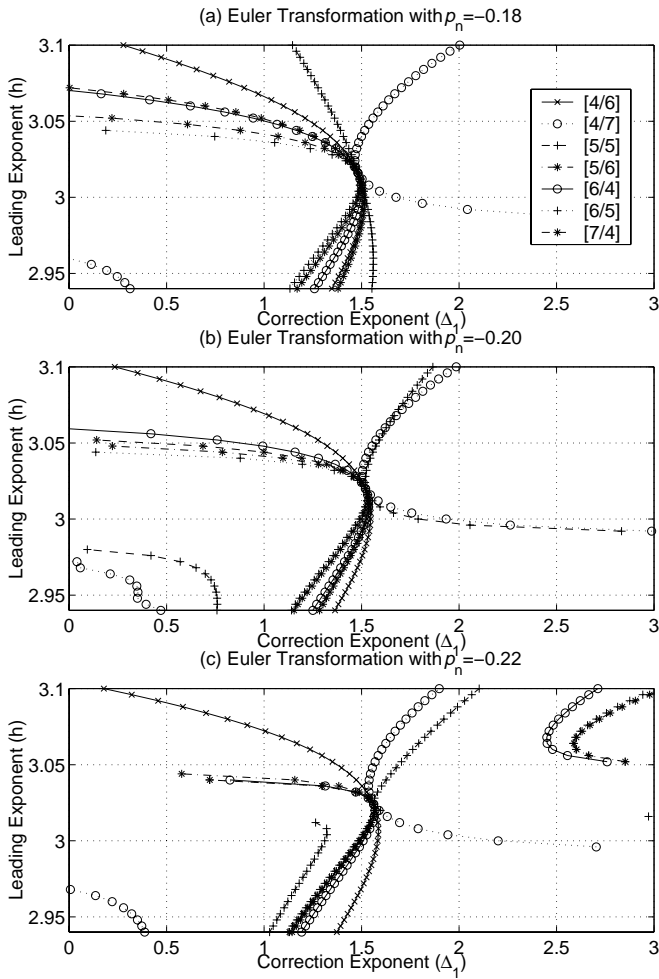


**Fig. 11.** Plots from an M1 analysis of the series  $A_4(p)/p$  for BQP ( $E = 0.05$ ) showing the influence of varying  $p_n$  in the Euler transformation. As can be seen from parts (a), (b), and (c), different  $p_n$ -values change the lines for individual Padé approximants, but keep the convergence point fixed.

There are however several other publications by independent research groups which give support to the observed behavior [11, 14, 17–20, 37–39]:

- Mookerjee *et al.* [11, 40] have listed most of the above references, including the methods which were used and the conclusions. Authors using real space renormalization (RSR), recursion methods (RM), or Thouless-Edwards-Licciardello boundary perturbation methods (TEL) found transitions with  $p_q$ -values ranging from 0.7 to 1 for either the site or the bond case.
- In addition, Srivastava and Chaturvedi [39] reported  $p_q = 0.73$  for SQP, based on equation of motion (EOM) methods.
- We also observe satisfactory numerical agreement on  $p_q$  estimates with other studies, by Koslowski *et al.* [20] and Raghavan [19] (his lower limit). Earlier estimates by Odagaki and Chang [17] are based on real space renormalization group calculations with very small cells, and hence may not be numerically reliable.

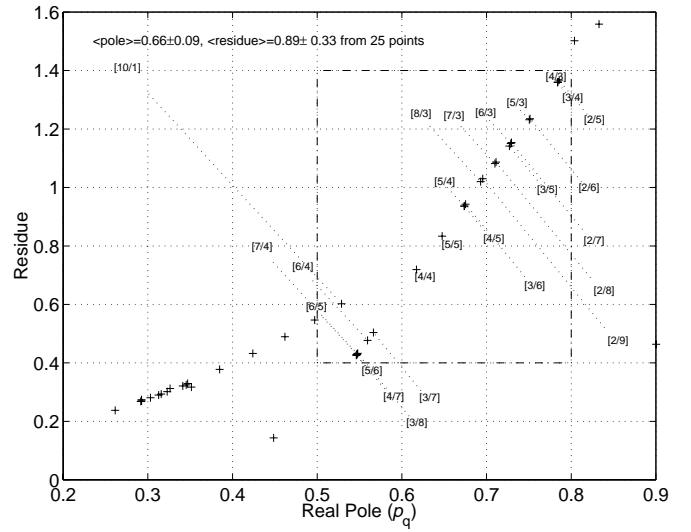


**Fig. 12.** Dlog-Padé analysis of the logarithmic derivative of  $A_2(p)/p$  of bond percolation, to check for an essential singularity. Although there are only a few data-points, they support the proposed power-law divergence as opposed to the exponential divergence (see text). The printed averages result from the points in the boxed region (the standard deviations are given as errors).

Thus, our results agree with the overwhelming majority of numerical studies of 2D QP on the existence of a transition from exponentially localized states to at most power law decaying states. The only real (pertaining) numerical disagreement comes from studies by Taylor and MacKinnon [16] and Soukoulis and Grest [7], based on the transfer matrix method applied to quasi one-dimensional strips of finite width combined with finite size scaling. The latter authors remark that *the transfer matrix technique and finite size scaling (FSS) is proven to be the most reliable technique*, but judging from comments by other authors [40] it also has its problems. Due to the underlying narrow strips, the possibility of an inbuilt one-dimensional geometry which influences the results cannot be ruled out.

Independent estimates for the supposedly universal localization exponent  $\nu$  (if one assumes a power law divergence of the localization length) are rare. Apart from series expansion we know only of the paper by Odagaki and Chang [17], who obtained  $\nu = 3.35$  for the site case and  $\nu = 1.89$  for the bond case, using RSR with the minimal cell size of  $2 \times 2$ . Our estimate for the localization length exponent  $\nu$  is in the range  $0.46 \dots 0.69$ . As already mentioned, these values violate the Chayes bound. (As mentioned before, this bound may not be applicable to QP.) Our result supports the possibility that quantum percolation may be in a different universality class than the Anderson model, for which there exists evidence that all states in 2D are localized.

Finally, we note that the existence of power law or weakly localized states is not particular to QP. Such states have also been observed for the 2D Anderson model by many authors, two of which we cite as examples.

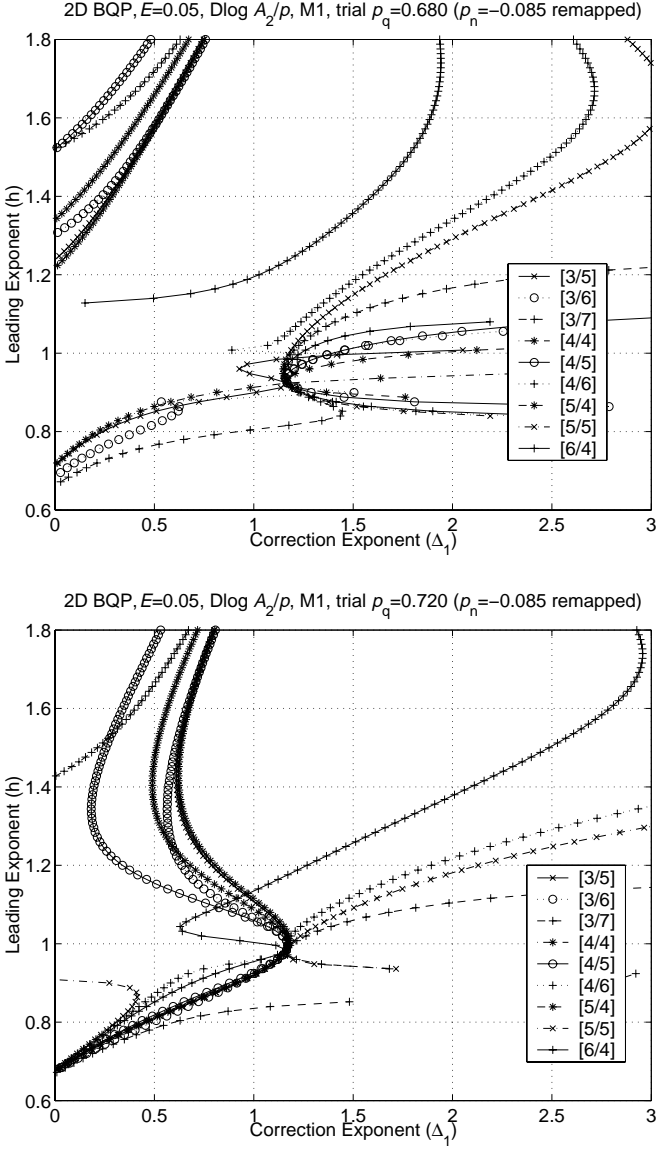


**Fig. 13.** M1 study of the logarithmic derivative of  $A_2(p)/p$  of bond percolation, to check for an essential singularity. Both parts show reasonable convergence near a leading exponent of 1 with a trial threshold near the proposed  $p_n$ . The slightly higher values for  $p_n$  may be due to the shortened series.

Kaveh [41] studied the model theoretically and gave experimental evidence for his predictions of non-metallic transport by quasi-extended wave-functions, which change into purely power-law decaying states for large length scales. He concludes that all the available data support the existence of power-law localized states which are separated by a mobility edge from exponentially localized states. Godin and Haydock [42,43] calculated the electronic transmittance as a function of energy using the block recursion method. They observed a sharp edge between weakly and strongly localized states near but well inside the band edge.

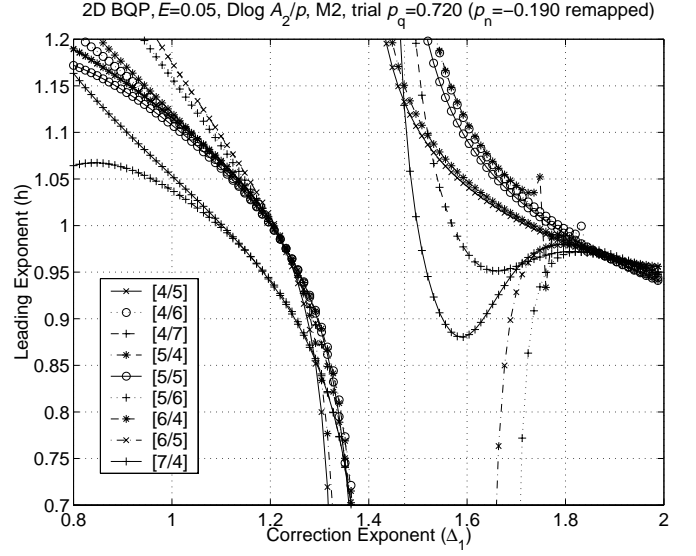


**Fig. 14.** M2-plot which is in agreement with the M1 study from Figure 13.

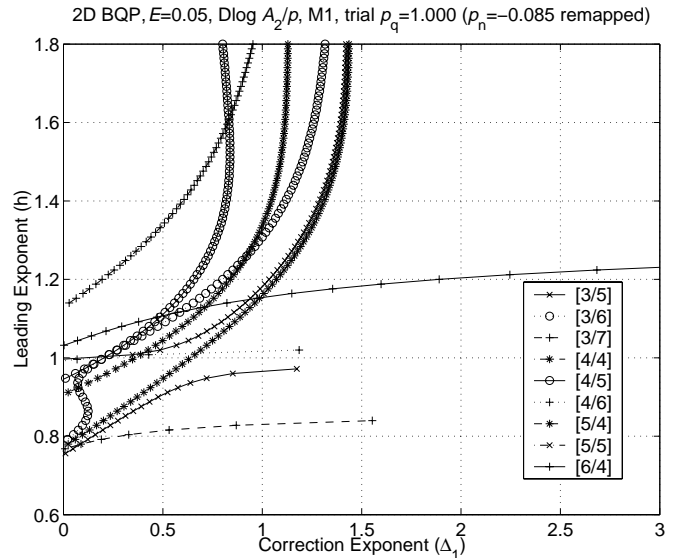


**Fig. 15.** M1 plot for the logarithmic derivative of  $A_2(p)/p$  of bond percolation at a trial- $p_q$  of 1. The absence of a convergence region does not support the possibility of the essential singularity.

We acknowledge discussions with Joan Adler, A. Brooks Harris, and Zvi Lev. We thank the German Israeli Foundation for support. I. C. also acknowledges a partial support from BSRI-98-2412 of the Ministry of Education, Korea.

## References

1. P.W. Anderson, Phys. Rev. B **109**, 1492 (1958).
2. P.A. Lee, T.V. Ramakrishnan, Rev. Mod. Phys. **57**, 287 (1985).
3. E. Abrahams, P.W. Anderson, D.C. Licciardello, T.V. Ramakrishnan, Phys. Rev. Lett. **42**, 673 (1979).
4. Y. Shapir, A. Aharony, A.B. Harris, Phys. Rev. Lett. **49**, 486 (1982).

5. Y. Meir, Ph.D. thesis, Tel Aviv University, 1988.
6. Y. Meir, A. Aharony, A.B. Harris, *Europhys. Lett.* **10**, 275 (1989).
7. C.M. Soukoulis, G.S. Grest, *Phys. Rev. B* **44**, 4685 (1991).
8. I. Dasgupta, T. Saha, A. Mookerjee, B.K. Chakrabarti, *AIP-Conference-Proceedings* **286**, 249 (1994).
9. I. Chang *et al.*, *Phys. Rev. Lett.* **74**, 2094 (1995).
10. I. Chang *et al.*, *J. Korean Phys. Soc.* **28**, S623 (1995).
11. A. Mookerjee, I. Dasgupta, T. Saha, *Int. J. Mod. Phys. B* **9**, 2989 (1995).
12. R. Berkovits, Y. Avishai, *Phys. Rev. B* **53**, R16125 (1996).
13. A. Kaneko, T. Ohtsuki, *J. Phys. Soc. Jpn* **68**, 1488 (1999).
14. M. Letz, K. Ziegler, *Philos. Mag. B* **79**, 491 (1999).
15. J.T. Chayes, L. Chayes, D.S. Fisher, T. Spencer, *Phys. Rev. Lett.* **57**, 2999 (1986).
16. J.P.G. Taylor, A. MacKinnon, *J. Phys. Cond. Matter* **1**, 9963 (1989).
17. T. Odagaki, K.C. Chang, *Phys. Rev. B* **30**, 1612 (1984).
18. K.C. Chang, T. Odagaki, *J. Phys. A* **20**, L1027 (1987).
19. R. Raghavan, *Phys. Rev. B* **29**, 748 (1984).
20. T. Koslowski, W. von Niessen, *Phys. Rev. B* **42**, 10342 (1990).
21. J. Adler *et al.*, *J. Stat. Phys.* **58**, 511 (1990).
22. D. Stauffer, A. Aharony, *Introduction to Percolation Theory* (Taylor and Francis, London, 1994).
23. D. Daboul, Ph.D. thesis, Tel Aviv University, 2000.
24. J.L. Martin, in *Phase Transitions and Critical Phenomena*, edited by C. Domb, M.S. Green (Academic Press, New York, 1974), Vol. 2, p. 97.
25. D.H. Redelmeier, *Discrete Mathematics* **36**, 191 (1981).
26. S. Redner, *J. Stat. Phys.* **29**, 309 (1982).
27. D. Daboul, A. Aharony, D. Stauffer, *J. Phys. A* **33**, 1113 (2000).
28. J.L. Gammel, in *Padé Approximants and Their Applications*, edited by B.R. Graves-Morris (Academic Press, New York, 1973).
29. J. Adler, M. Moshe, V. Privman, *Phys. Rev. B* **26**, 1411 (1982).
30. J. Adler, I. Chang, S. Shapira, *Int. J. Mod. Phys. C* **4**, 1007 (1993).
31. J. Adler, D. Stauffer, *Physica A* **181**, 396 (1992).
32. M. Gofman *et al.*, *Phys. Rev. Lett.* **71**, 1569 (1993).
33. J. Adler, I.G. Enting, *J. Phys. A* **17**, 2233 (1984).
34. C.J. Pearce, *Adv. Phys.* **27**, 89 (1978).
35. A. Aharony, A.B. Harris, *Physica A* **191**, 365 (1992).
36. C.M. Soukoulis, E.N. Economou, G.S. Grest, *Phys. Rev. B* **36**, 8649 (1987).
37. S.N. Evangelou, *Phys. Rev. B* **27**, 1397 (1983).
38. M. Chaturvedi, V. Srivastava, *Phys. Stat. Sol. B* **120**, 421 (1983).
39. V. Srivastava, M. Chaturvedi, *Phys. Rev. B* **30**, 2238 (1984).
40. A. Mookerjee, B.K. Chakrabarti, I. Dasgupta, T. Saha, *Physica A* **186**, 258 (1992).
41. M. Kaveh, *Phil. Mag. B* **52**, 521 (1985).
42. T.J. Godin, R. Haydock, *Europhys. Lett.* **14**, 137 (1991).
43. T.J. Godin, R. Haydock, *Phys. Rev. B* **46**, 1628 (1992).